

# Test and simulation of High-Tc superconducting power charging system for solar energy application

Haeryong Jeon<sup>a</sup>, Young Gun Park<sup>a</sup>, Jeyull Lee<sup>a</sup>, Yong Soo Yoon<sup>\*b</sup>, Yoon Do Chung<sup>c</sup>, and Tae Kuk Ko<sup>a</sup>

<sup>a</sup> Yonsei University, Seoul, Korea

<sup>b</sup> Shin Ansan University, Ansan-si, Korea

<sup>c</sup> Suwon Science College, Suwon-si, Korea

(Received 7 August 2015; revised or reviewed 20 September 2015; accepted 21 September 2015)

## Abstract

This paper deals with high-Tc superconducting (HTS) power charging system with GdBCO magnet, photo-voltaic (PV) controller, and solar panels to charge solar energy. When combining the HTS magnet and the solar energy charging system, additional power source is not required therefore it is possible to obtain high power efficiency. Since there is no resistance in superconducting magnet carrying DC transport current the energy losses caused by joule heating can be reduced. In this paper, the charging characteristics of HTS power charging system was simulated by using PSIM. The charging current of HTS superconducting power charging system is measured and compared with the simulation results. Using the simulation of HTS power charging system, it can be applied to the solar energy applications.

*Keywords:* HTS, Solar energy, Power charging system, GdBCO magnet, Flux pump, Heater triggered switch

## 1. INTRODUCTION

The use of fossil energy generates large quantity of CO<sub>2</sub> that have been known for major causes of global warming and climate change. Solar energy have been developed as electrical energy sources instead of fossil energy. Solar cell directly produces electrical energy by using photoelectric effect. Solar energy is infinite energy sources, and the energy is environmentally friendly [1]. However, solar energy has disadvantages that can't be used when there is no solar radiation such as during night and rainy weather. For this reason, Energy Storage System (ESS) is needed for flexible use of solar energy. Most of the solar energy systems use a battery in order to store the energy. The battery is easy to use, and there is an advantage that the amount of charge per area is large. However, long charging time and conversion loss is disadvantages of the battery. High-Temperature Superconducting (HTS) power charging system have been studied to overcome these disadvantages [2]. The HTS magnet stores electrical energy, and the stored electrical energy is operated in persistent current mode. The commercial power source can be replaced with HTS power charging system combined with solar energy system. The charging energy density of the HTS power charging system is low compared with the other energy storage device such as the battery. But the system have a high transform energy efficiency [3].

In this paper, we implemented the charging tests using the GdBCO magnet, and the system was simulated by using PSIM 9.0 based on the experimental parameters PSIM 9.0 based on the experimental parameters.

\* Corresponding author: [ysyoon@sau.ac.kr](mailto:ysyoon@sau.ac.kr)

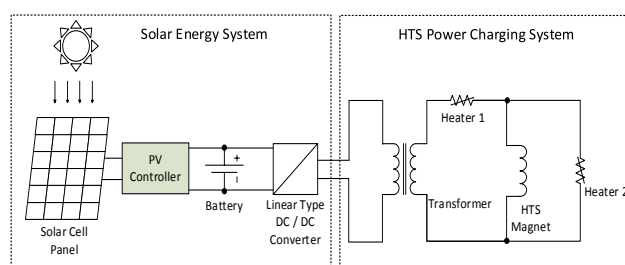


Fig. 1. Schematic diagram of HTS power charging system combined with solar energy system.

Heater-triggered switches that is wound with the HTS tape are used to make a flux pump. The flux pump has two different types, rotation and transformer type. The transformer type of flux pump that is more efficient than rotation type is used in this charging tests. This flux pump converts the magnetic energy to electrical energy, and this energy is used to the load. The PSIM simulation shows results that how much electrical energy is stored and how much charging time is needed. The critical factors to design the HTS power charging system is investigated by simulation.

## 2. CONCEPT OF HTS POWER CHARGING SYSTEM COMBINED WITH THE SOLAR ENERGY SYSTEM

### 2.1. System structures

Fig. 1 shows the schematic diagram of the entire system. It consist of two major parts as follow;

TABLE I  
SPECIFICATIONS OF THE HTS POWER CHARGING SYSTEM.

Parameter	Specification
<b>HTS magnet (Double pancake magnet)</b>	
Material	GdBCO
Inner / Outer diameter	80 / 202 mm
Number of turns	$240 \times 2 = 480$ turns
Inductance	32mH
Total length	200m
Critical current	65 A
<b>Transformer (Primary)</b>	
Coil material	Copper wire (1.2 mm)
Number of turns	240 turns
Core material	Carbon steel
<b>Transformer (Secondary)</b>	
Material	GdBCO
Number of turns	10 turns
Core material	Carbon steel
<b>Heater 1 and 2</b>	
Material	Nickel-Chrome alloy
Wire diameter	0.203 mm
Resistance	35 $\Omega$ , respectively

TABLE II  
SPECIFICATIONS OF THE SOLAR ENERGY SYSTEM.

Parameter	Specification
<b>PV module</b>	
mpp voltage (V)	24.1
mpp current (A)	7.24
Maximum system voltage (V)	1000
Thickness of cell (mm)	4
Operating life (year)	90
Dimensions (L $\times$ W $\times$ H) (mm)	651 $\times$ 986 $\times$ 46
<b>PV controller</b>	
Rated solar current (A)	30
Rated load current (A)	30
System voltage (V)	12, 24
Dimensions (L $\times$ W $\times$ H) (mm)	170 $\times$ 90 $\times$ 35
<b>Battery</b>	
Current (A) / period of the usable power (hour)	5 / 45 15 / 12 25 / 7
Dimension (L $\times$ W $\times$ H) (mm)	330 $\times$ 170 $\times$ 210
<b>DC-DC converter</b>	
Control range voltage (mV)	0 ~ 5000
Resolution power	1mV $\times$ 1mA
Control range current (mA)	-6000 ~ 6000
Switching time (ms)	Below 20

### 1) Solar Energy System

### 2) HTS Power Charging System

Solar energy system is categorized as stand-alone type and grid-connected type [3]. Stand-alone type of the solar energy system is used in the tests. Solar energy is converted to electrical energy by using the solar cell array

and this electrical energy is charged to the battery through the Photovoltaic (PV) controller. Maximum Power Point Tracking (MPPT) control finds the optimum operating point of the irregular voltage depending on the amount of solar radiation [4]. Solar energy charged to the 24 V batteries and DC-DC linear converter converts voltage to test voltage using pulse width modulation (PWM). It is charged to the HTS power charging system through the transformer.

### 2.2. Solar Energy System

Solar energy system consists of solar cell array, PV controller, batteries and DC-DC converter. Its specifications are noted in TABLE II. The solar cell array is tilted the angle of 30° to maximize power generation efficiency [1].

The PV controller controls the electrical energy which is converted from solar cell arrays. The electrical energy is charged to the battery through the PV controller. There is a function to protect the circuit during overcurrent situation. PV controller is possible to monitor how much current flows during charging operation [3].

Electrical energy is not uniformly generated from the solar cell. Generated power is depends on position of the solar radiation and solar intensity. So, electrical energy is charged to the battery for the same conditions of experiments during charging tests. DC-DC converter converted magnitude of current, and which make time varying current in order to link to the transformer.

### 2.3. HTS Power Charging System

HTS power charging system consists of GdBCO magnet, transformer and heater-triggered switches. The transformer amplifies the current which came out from DC-DC converter. Primary current is transformed to the magnetic flux and linked to the secondary coil. The more the magnetic flux is linked to the secondary coil, the more pumping current is charged to the GdBCO magnet. The ratio of the primary and the secondary winding is 240:10 in order to increase the magnetic flux into the secondary side. Carbon steel material is used to core of the transformer in the tests.

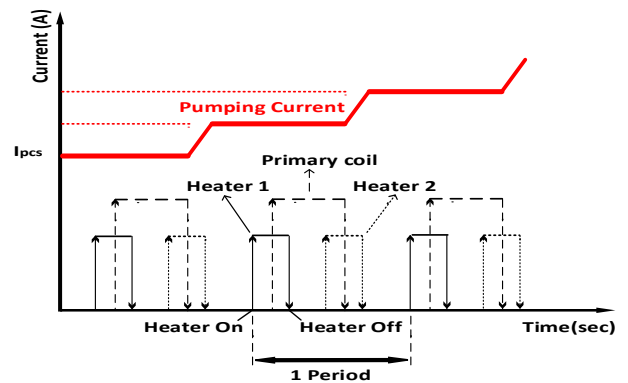


Fig. 2. Schematic diagram for pumping current.

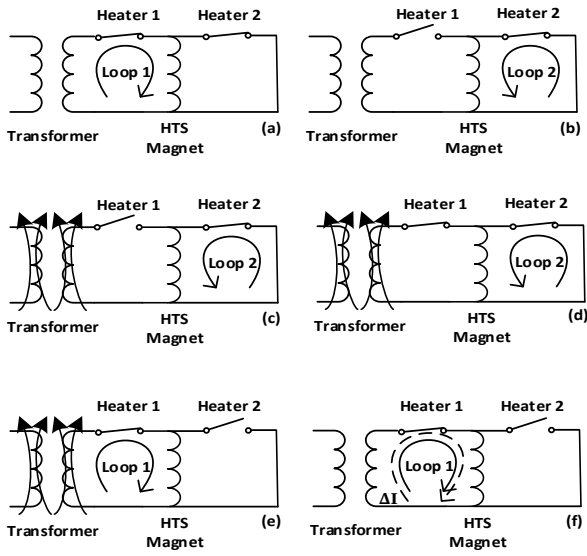


Fig. 3. Charging sequence of the GdBCO magnet by heater-triggered switch.

Heater-triggered switch utilizes quench characteristic that superconductor's resistance become almost infinite in situation that superconductor's temperature is over the critical temperature [5]. Fig. 2 is a schematic diagram for pumping current, and Fig. 3 is a diagram of the charging sequence. The magnetic flux is applied to the secondary coil of the transformer by the primary current (c). The heater-triggered switch 1 is turned on (d), and switch 2 is turned off (e), then closed loop1 is formed (e). At this time, the primary current is turned off (f). So, the pumping current generated by the reduced magnetic flux because of the Faraday's law (f). This pumping current is charged to the GdBCO magnet until the current is saturated.

### 3. TEST AND SIMULATION OF THE HTS POWER CHARGING SYSTEM

#### 3.1. Test of the HTS power charging system

The 24 V battery is charged by using the solar cell array and the PV controller. This electrical energy converted to HTS power charging system through the DC-DC linear convert and the transformer. HTS power charging system part is immersed in liquid nitrogen to cool down the

TABLE III  
CURRENT AND TIME CHART OF THE CHARGING SEQUENCE.

	Mode 1	Mode 2	Mode 3
Primary Current	12A	12A	9A
Heater1 On Time	0.3s	0.5s	0.3s
Heater 1 Off Time	1.8s	3s	5.5s
Heater 2 On Time	2.7s	4.5s	8.3s
Heater 2 Off Time	4.2s	7s	13.5
Primary current On Time	1.2s	2s	3s
Primary current Off Time	3.6s	6s	11s
Period	4.5s	7.5s	15s

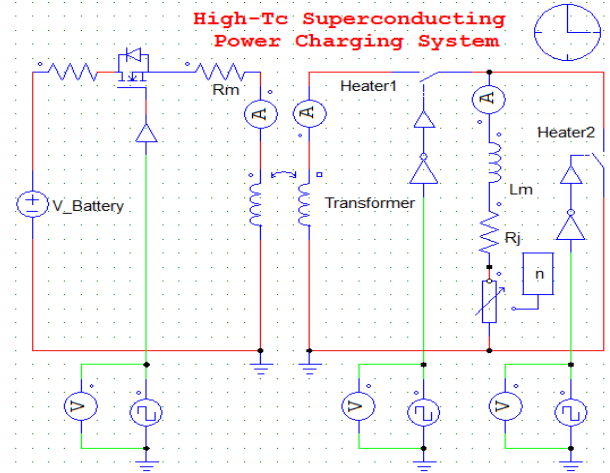


Fig. 4. Circuit diagram of the HTS power charging system.

superconductors. The tests was performed under different switching conditions in order to get the design parameters. TABLE III shows test conditions of the switching sequences and magnitude of current.

#### 3.2. Simulation of the HTS power charging system

Fig. 4 shows diagram of power charging simulation by using PSIM 9.0. One of the design parameter is transformer's self-inductance and mutual-inductance. Ideal transformer model in PSIM is not possible to design the amount of inductance during the current excitation. Charging current in the magnet appears nonlinear characteristics during current saturation in the magnet. As follows formulation explains the saturation characteristics.

$$V_c = E_c l \left( \frac{I}{I_c} \right)^n \quad (1)$$

$E_c$  is the electric field defining critical current in 0.1  $\mu\text{V}/\text{cm}$  [6].

Index value "n" can be determined based on the measured value when the magnet is quench [7].

TABLE IV  
ELECTRICAL PARAMETERS FOR THE SIMULATION.

Symbol	Quantity	Value
$L_m$	HTS Magnet inductance	32mH
$R_j$	Joint resistance	1.38 $\mu\Omega$
n	Index number	17
$E_c$	Electric field in HTS magnet	0.1 $\mu\text{V}$
l	Total length	200m
$I_c$	Critical current of HTS magnet	65A
$L_1$	Primary copper winding self-inductance	7.76mH
$L_2$	Secondary copper winding self-inductance	0.155mH
$M_1$	Mutual inductance between L1 and L2	1.08mH
$M_2$	Mutual inductance between L1 and $L_m$	0
$M_3$	Mutual inductance between L2 and $L_m$	0
$R_m$	Primary copper winding resistance	0.08 $\Omega$

$$n = \frac{\ln(E_2/E_1)}{\ln(I_2/I_1)} \quad (2)$$

$I_1$  and  $E_1$  is a current and the electric field when quench begins to occur at the GdBCO magnet.  $I_2$ ,  $E_2$  is a current and the electric field after the voltage has risen at the GdBCO magnet.

Joint resistance is calculated by discharging test of persistent current mode.

$$R_j = \frac{L_m}{T_E - T_I} \times \log\left(\frac{I_E}{I_I}\right) \quad (3)$$

$T_I$  is the initial time of the persist current mode and  $T_E$  is the end time of the persistent current mode.  $I_E$  is the end current and  $I_I$  is the initial current value [6].

TABLE IV explains the electrical parameters for the simulation. The values of the parameter are the same as the HTS power charging system which has been used in the experiments. The experiment results and the simulation results are compared to verify reliability. And the charging test is simulated different mutual inductance and different index value to find critical factor which affects to pumping current and saturation current.

#### 4. RESULTS

Fig. 5 (a) shows the test results of different charging conditions of TABLE III. The magnet current started saturation from above 50 A. The current of Mode 1 started saturation at 1,200seconds and converged to 55.7 A. The current of Mode 2 converged to 56.4 A with saturated from 2,000 seconds. In the case of Mode 3, the charging current is 29 A and the magnet is unsaturated until at 3,500seconds. If charging time becomes long, charging current of Mode 3 will be converged to some value.

Fig. 5 (b) shows the pumping current of Mode 2 graph during 5 period. Charging current of magnet is increased 0.41 A at one period. Mode 1 is also almost same pumping current about 0.42 A because primary current is same with Mode 1.

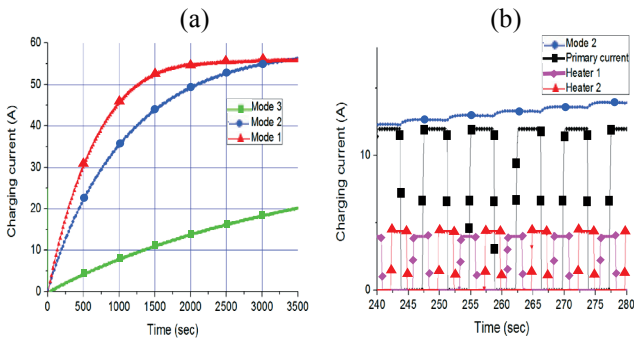


Fig. 5. Test results of pumping current under different current and switching sequences (a). Operating results of charging test at Mode2 (b).

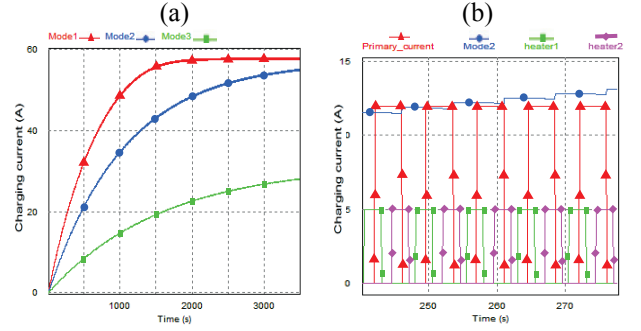


Fig. 6. Simulation results of pumping current under different current and switching sequences (a). Simulation results of charging test at Mode2 (b).

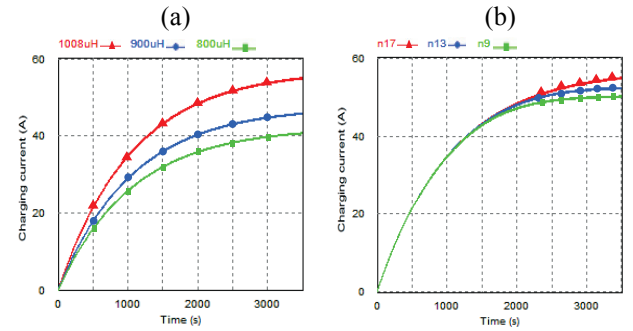


Fig. 7. Simulation results of pumping current under different mutual inductance (a) and different index value (b)

The PSIM simulation results are drawn as shown in Fig. 6. Mode 1 started saturation at 1,300seconds and converged to 57 A. The current of Mode 2 and Mode 3 converged to 54.5 A and 28 A respectively. The simulations have error that is under 4% in the same parameters. Fig. 6 (b) shows the simulation results of Mode 2 graph during 5 period. Simulation of Mode 2's pumping current is about 0.40 A that value is almost same with experimental result for Mode 2.

The charging simulation is implemented according to the mutual inductance of the transformer. Fig. 7 (a) shows the result of simulation that mutual inductance is 1008  $\mu$ H, 900  $\mu$ H and 800  $\mu$ H respectively. The mutual inductance of the transformer determined by the magnetizing inductance and the leakage inductance. So, it can be seen that the quantity of pumping current is decreased according to the decreasing mutual inductance. Fig. 7 (b) is a simulation result of the current saturation curve according to the index value that is  $n=17$ ,  $n=13$  and  $n=9$  respectively. The saturation current is changed to 54.5 A, 52.3 A and 50.1 A According to the index value. It was described by the formulation (1) that the saturation time of the current in the magnet is determined by the index value.

#### 5. CONCLUSION

Much of cost and time is needed to manufacture the HTS

power charging system. So, simulation of the HTS power charging system is important pre-processing to optimize cost and time. In this paper, HTS power charging system is designed for solar energy system. Saturating current and charging time is compared as different switching sequences and different current throughout the experiments. Also HTS power charging system is simulated by using PSIM. Reliabilities of simulation are verified by comparing simulation results and experiment results. Maximum charging current and charging time of HTS power charging system can be calculated by implementing a non-linear characteristic on simulation. Saturation current and full charging time is changed according to switching time and primary current during pumping sequences. And we simulated the charging time and the saturation current that is affected by index value and mutual inductance. We plan to analyze the error rate and reliability throughout the test and simulation at the discharge sequences.

#### ACKNOWLEDGMENT

This work was supported by the Basic Science Research Program through the National Research Foundation of Korea (NRF) funded by the Ministry of Education (Grant 2011-0009232).

#### REFERENCES

- [1] Dong-Jin Choi, "Comparison Researches for Installation of the Module Angles and Array Spacing on Photovoltaic Power System," *KIIEE*, vol. 23, no. 1, pp. 162-168, 2009.
- [2] Y. Do Chung, D. W. Kim, H. C. Jo, Y. S. Yoon, H. K. Kim, and T. K. Ko, "Fundamental performance of novel power supply for HTS magnet using solar energy system," *Cryogenics*, vol. 51, no. 6, pp. 220-224, 2011.
- [3] Dae Wook Kim, Yoon Do Chung, Hyun Chul Jo, Yong Soo Yoon, Hyun Ki Kim, Tae Kuk Ko, "Fabrication and Test of HTS Flux Pump Combined with Solar Energy System," *Progress in Superconductivity and Cryogenics*, vol. 13, no. 1, pp. 22-26, 2011.
- [4] Dae Wook Kim, Yong Soo Yoon, Yoon Do Chung, Hyun Chul Jo, Ho Min Kim, Tae Jung Kim, Jae Gi Oh, Tae Kuk Ko, "Characteristic Analysis of HTS Magnet Charging System Combined with PV System Using MPPT Control," *Progress in Superconductivity and Cryogenics*, vol. 14, no. 1, pp. 8-13, 2012.
- [5] H. C. Jo, Y. G. Park, Y. Do Chung, H. M. Kim, T. K. Ko, and Y. S. Yoon, "Design and Test of a High-Tc Superconducting Power Conversion System With the GdBCO Magnet," *IEEE Trans. Appl. Supercond.*, vol. 24, no. 3, pp. 1-5, 2014.
- [6] Y. S. Yoon, H. C. Jo, Y. G. Park, J. Lee, K. Y. Yoon, H. Kim, Y. Do Chung, Y. Chu, and T. K. Ko, "Analysis of a High-Tc Superconducting Power Converting System," *IEEE Trans. Appl. Supercond.*, vol. 25, no. 3, pp. 2-5, 2015.
- [7] Y. S. Yoon, H. M. Kim, M. Joo, D. K. Bae, M. C. Ahn, and T. K. Ko, "Characteristics analysis of a high-Tc superconducting power supply considering flux creep effect," *IEEE Trans. Appl. Supercond.*, vol. 16, no. 3, pp. 1918-1923, 2006.